Available online at www.sciencedirect.com
SCIENCE DIRECT
EPSL
Earth and Planetary Science Letters 217 (2004) 367–378
www.elsevier.com/locate/epsl

Thermal, hydrous, and mechanical states of the mantle transition zone beneath southern Africa

John Blum [a,*], Yang Shen [b]

[a] Institute of Geophysics and Planetary Physics, Scripps Institution of Oceanography, University of California – San Diego, 9500 Gilman Drive, La Jolla, CA 92093-0225, USA

[b] Graduate School of Oceanography, University of Rhode Island, South Ferry Road, Narragansett, RI 02882, USA

Received 16 April 2003; received in revised form 15 October 2003; accepted 24 October 2003

Abstract

Observations of P-to-S conversions from the seismic discontinuities near 410 and 660 km depth reveal the shoaling of the 410-km discontinuity and the deepening of the 660-km discontinuity beneath the Archaean cratons in southern Africa; consequently, the mantle transition zone is 20 km thicker than beneath post-Archaean regions and the global average. The discontinuity structure, combined with tomographically imaged seismic velocities, suggests a relatively cold ($\Delta T \sim 100$ K) and water-enriched (ΔOH $\sim$ 20–35% saturation) transition zone beneath the cratons. The thicker-than-normal transition zone correlates with surface geology and does not follow the track of African plate motion as numerical simulations of small-scale convection imply. The observations suggest that cold thermal downwelling is not the primary cause of the anomalously thick transition zone beneath the cratons, although it may exist in a confined area near the boundary between the Kheis thrust belt and the Namaqua-Natal belt. If thermal downwelling exists, its temperature anomaly at the 660-km discontinuity must be below the levels detectable by the method used in this study ($\Delta T \sim 60$ K). The spatial correlation between surface geology, high velocities beneath the cratons, and the transition zone structure indicates that the cratonic keels extend to the base of the upper mantle, substantially deeper than most estimates. Our results demonstrate the need to closely consider the effect of water content on seismic velocities beneath deep continental roots.

Keywords: lithosphere; upper mantle; transition zone; cratoni convection; Southern Africa

1. Introduction

The upper mantle beneath southern Africa occupies an interesting place between a deep mantle upwelling and the Archaean continent. The high uplifted topography of Africa has been attributed to the upwelling of an anomalously hot mantle [1]. Global tomographic studies have confirmed the presence of a large-scale, low-seismic-velocity anomaly deep within the mantle [2,3]. The prominent low-velocity anomaly is more than 1000 km wide and rises upwards near 1500 km from the core–mantle boundary. A high-attenuation anomaly in the mantle transition zone beneath Africa,

* Corresponding author. Tel.: +1-858-922-4975; Fax: +1-858-534-5332.

E-mail addresses: johnblum@ucsd.edu (J. Blum), yshen@gso.uri.edu (Y. Shen).

0012-821X/03/$ – see front matter © 2003 Elsevier B.V. All rights reserved.
doi:10.1016/S0012-821X(03)00628-9

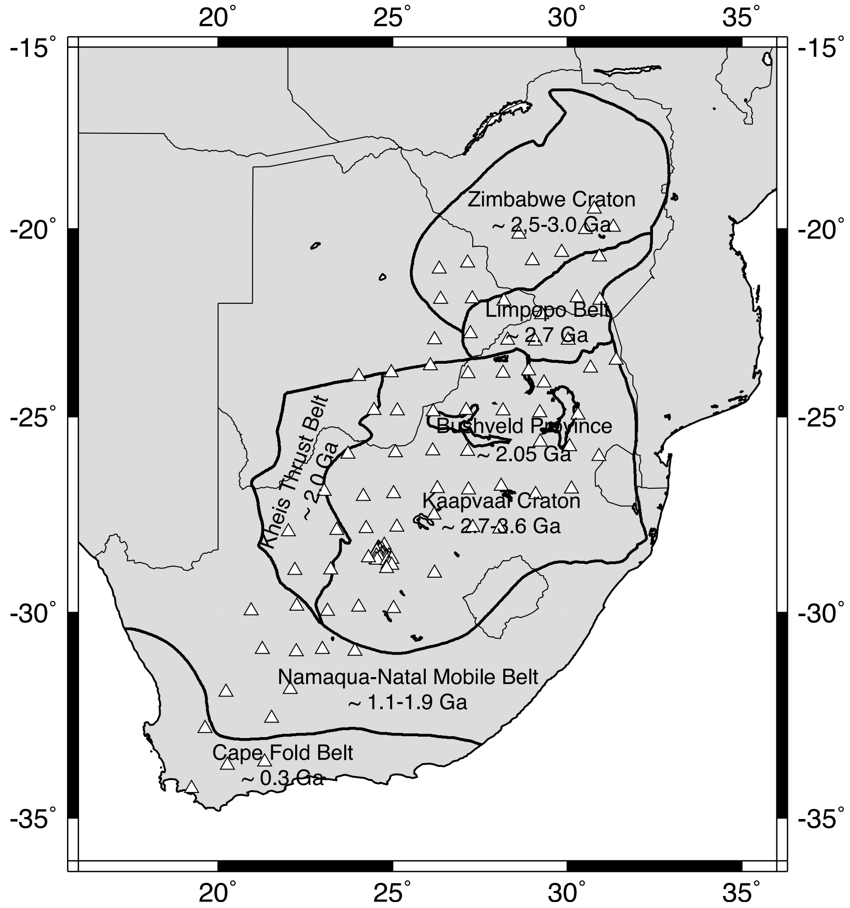

Fig. 1. Locations of broadband seismic stations (triangles) and geologic provinces in southern Africa. The temporary seismic networks comprised the Kaapvaal project [15,16] and Kimberley array and included 113 sites. The networks operated from April 1997 to July 1999 and from December 1998 to July 1999, respectively, and extended from Cape Town, South Africa, to regions of Zimbabwe and Botswana.

imaged by waveform tomography, is interpreted as evidence that thermal upwelling associated with the low-velocity structure in the lower mantle persists through the upper mantle transition zone [4].

Near the surface, the South African lithosphere encompasses extensive Archaean cratons (Fig. 1), which formed under conditions unique to the Archaean, including a rapid series of tectonic processes involving magmatism and subduction [5,6]. As a result, the cratons are believed to possess unique chemical and physical characteristics compared to the post-Archaean continent. These characteristics include low heat flow [7], a composition of highly depleted peridotites [8], and a high-seismic-velocity keel that extends to depths of 200 km or deeper [9]. Questions remain regarding the true depth of the continental roots beneath southern Africa and elsewhere [10–12] and their role in continental evolution.

One possible role of continental keels is their effect on small-scale convection in the upper mantle. Numerical simulations predict cold thermal downwellings in the upper mantle adjacent to craton margins, where significant thermal contrast exists [13,14]. The relatively slow motion of the African plate and the large thermal contrast between the Archaean cratons and the oceanic lithosphere make southern Africa an ideal study area to search for small-scale downwellings adjacent to craton boundaries. While global tomography supports the notion of edge-driven downwellings flanking the south African cratons [12,14], a systematic seismic investigation of small-scale convection on the regional scale has yet to be performed.

Recent broadband seismic experiments in southern Africa collected a large volume of seismic data to characterize the upper mantle beneath the study area. High-velocity features have been verified to depths of at least 250 km, and perhaps up to 300 km in local regions beneath the cratons [15,16]. At greater depth, the spatial correlation between high-velocity anomalies and the cratons breaks down. This can be explained either by a limited depth extent of the continental keel or, as evidence presented in this paper indicates, by an increasing importance of compositional effects on seismic velocity in the deep mantle.

The thermal state of the mantle transition zone can also be constrained by mapping the mantle discontinuities near 410 and 660 km depth, which correspond to the phase transitions from α-olivine to β-spinel (wadsleyite) and from γ-spinel (ringwoodite) to (Mg,Fe)SiO_3-perovskite plus (Mg,Fe)O-magnesiowüstite [17,18], respectively. The positive and negative Clapeyron slopes of the 410- and 660-km discontinuities, in that order, dictate a thinning of the mantle transition zone in the presence of thermal upwelling. For the same reason, a cold thermal anomaly penetrating the transition zone induces a thicker-than-normal transition zone [19]. Compositional variations in the transition zone, such as water content, may also affect the transition zone structure. Examining the transition zone thickness can thereby shed insight into the mantle structure and geophysical processes beneath southern Africa.

Using P-to-S conversions from roughly 1300 seismograms, Gao et al. [20] determined that the mean transition zone thickness beneath the study area is about the same as the global average. They suggested that the transition zone is not anomalously hot, in disagreement with the inference from the attenuation structure in the transition zone [4]. To reconcile this controversy and to obtain additional constraints on the depth of the cratonic roots and the role of cold thermal downwellings in the upper mantle bordering the cratons, we carried out further investigation of the mantle transition zone beneath the study area using a substantially greater number of useful seismic arrivals (∼3350 seismograms) than in the previous study. We removed the effect of lateral velocity heterogeneity on the waveforms to obtain a more coherent stacking of the converted phases from upper mantle discontinuities. We documented the shoaling of the 410-km discontinuity and the deepening of the 660-km discontinuity beneath the oldest parts of the Archaean cratons. The relation between the transition zone discontinuities and tomographically imaged seismic velocities [15,16], which were unavailable in the study by Gao et al. [20], reveals the presence of excess water in a relatively cold mantle transition beneath the Archaean cratons. Furthermore, the spatial correlation between surface geology, high velocities beneath the cratons, and the transition zone structure strongly indicates that the continental keels beneath southern Africa extend to the transition zone, substantially deeper than previously suggested.

2. Data processing and signal analysis

We used teleseismic body waves recorded by two temporary seismic networks in southern Africa (Fig. 1) to detect the conversion of compressional waves to shear waves at upper mantle seismic discontinuities (P_ds, where d stands for depth). The networks were deployed as part of the Kaapvaal experiment [15,16] and Kimberley array from April 1997 to July 1999, and from December 1998 to July 1999, respectively. The networks included more than 100 seismic stations extending from Cape Town, South Africa, to regions of Zimbabwe and Botswana. We inspected waveforms representing 283 teleseismic earthquakes of magnitude 5.5 and greater. The waveforms were windowed between 80 s before the P-wave arrival and 5 s before the PP arrival and were filtered using a two-pass Butterworth filter. Filtered waveforms having noise levels less than 0.1 times the amplitude of the direct P-wave on the vertical component were selected for analysis. We defined noise levels as the standard deviation of the radial values in the 80-s window preceding the P-wave arrival. The vertical P-wave components were deconvolved from the radial components to produce the radial receiver functions, which isolate the S energy converted from the incident P energy [21,22]. We selected a total of 3354 radial receiver functions for analysis, ~2.5 times the number used in the previous study of Gao et al. [20].

Significant lateral variations exist in both the crustal thickness and mantle velocities beneath the study area [23,15,16]. To account for these variations, we used multi-channel waveform cross-correlation [24] to measure relative travel time delays across the seismic networks and averaged them for each station in 10° azimuthal bins. We assumed that relative travel time delays across the array are due primarily to velocity heterogeneity in the crust and the upper 400 km of the mantle. The azimuthally dependent delays served as a first-order approximation to correct receiver functions for velocity heterogeneity in the crust

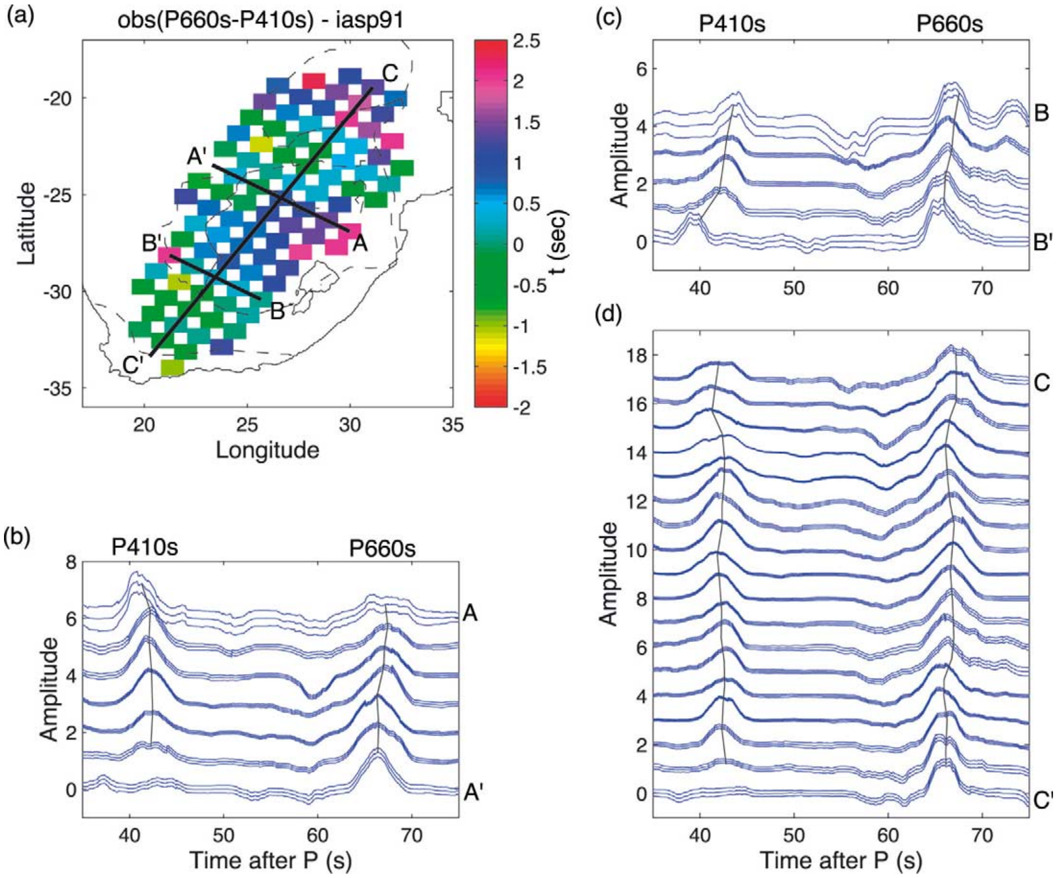

Fig. 2. (a) The map view displays variations in transition zone thickness with respect to the iasp91 model. A 1-s change in differential time is equivalent to about a 10-km change in the transition zone thickness. Dashed lines outline the boundaries of the geological provinces shown in Fig. 1. (b) Waveforms of the stacked receiver functions along the profile A–A′ in panel a and their 95% confidence limits estimated by bootstrap. Arrival times of P410s and P660s are connected across the traces. Amplitudes are relative, because non-linear stacking does not preserve amplitudes. (c) Waveforms of the stacked receiver functions along the profile B–B′. Correlated changes in P410s and P660s times reflect remaining velocity heterogeneity in the crust and upper 400-km mantle, where the two phases have nearly identical paths. (d) Waveforms of the stacked receiver functions along the profile C–C′.

and mantle beneath the stations with respect to predicted P_ds arrival times from the iasp91 global model [25].

Because the amplitude of the P-to-S conversions at the upper mantle seismic discontinuities was only a few percent of the incident P-wave, we stacked the waveforms to improve the quality of the signal (P_ds). We split the study area into an array of overlapping circular bins. To ensure signal quality, we only analyzed bins having at least 64 traces in the transition zone, so that the noise levels in the stacked receiver functions ($\sim$0.01 or less times the amplitude of P-wave on the vertical component in linear stacks) are several times lower than the amplitude of the converted phases from the transition zone discontinuities. We compared the results from 2°- and 1°-radius bins and we chose 2° bins in order to maximize spatial coverage while maintaining signal quality. Receiver functions of P_ds paths piercing the same bin at a given depth in the mantle were gathered and stacked [26,27] using an *n*th root ($n = 2$) stacking process [28]. The non-linear stacking process enhanced coherent signals and suppressed random noise. We used a bootstrap resampling method [29] to determine the arrival times of the signals in stacked traces and their 95% confidence limits.

3. Results

The stacked receiver functions (Fig. 2) show clear arrivals from the 410- and 660-km discontinuities (P410s and P660s, respectively), as well as a negative polarity phase from a seismic discontinuity near 590 km depth [30]. Variations in transition zone thickness – or the difference between the observed P660s–P410s differential times and the predicted iasp91 values [25] – reveal distinct differences between the early Archaean cratons and later formed terrains (Figs. 2 and 3). The transition zone beneath the Zimbabwe and Kaapvaal cratons is thicker than in the iasp91 model

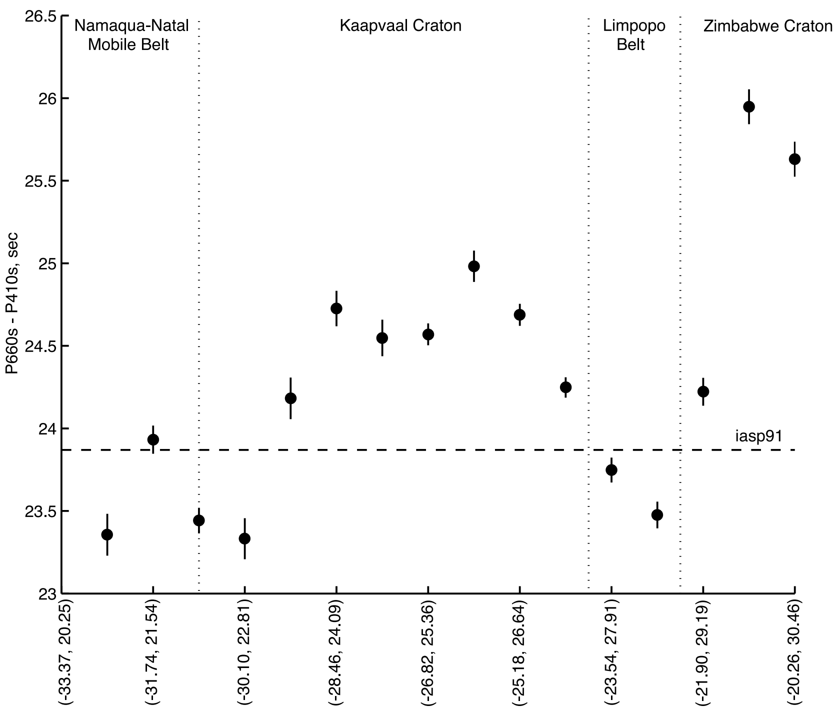

Fig. 3. Observed P660s–P410s times and uncertainties (1σ) across transect C–C′ in Fig. 2a. The iasp91 predicted differential time and approximate geologic boundaries are shown with dashed and dotted lines, respectively.

and the global average by up to 20 km. Lateral velocity heterogeneity in the transition zone [15,16] introduces ±2-km variation in the apparent transition zone thickness, within the uncertainty caused by receiver function noise. The thicker-than-normal transition zone correlates with patches of high-velocity anomalies that extend to at least 250 km depth [15,16]. A transition zone of normal value appears between the two cratons, coinciding surficially with the Bushveld province. A marginally thinner-than-normal transition zone exists at the post-Archaean Namaqua-Natal and Cape Fold belts, which correlates with a relatively thin lithosphere [15]. A notable exception is a thicker-than-normal transition zone near the boundary between the Kheis thrust belt and the Namaqua-Natal belt.

The P660s–P410s differential time varies laterally by up to 3.0 ± 0.5 s. This corresponds to a ∼30 ± 5-km difference in transition zone thickness from the Cape Fold belt to the nearby cratons. Fig. 2b–d shows SSE–NNW and NNE–SSW transects of the stacked receiver functions. With the exception of the anomaly at the boundary between the Kheis thrust belt and the Namaqua-Natal belt, P410s and P660s times are anti-correlated in areas with a thickened transition zone (Figs. 2 and 4). Anti-correlation of the P_ds phases suggests that the thickening of the transition zone beneath the cratons results from both the shoaling of the 410-km discontinuity and the deepening of the 660-km discontinuity. At the boundary between the Kheis thrust belt and the Namaqua-Natal belt, the large reduction in P410s time and the lack of increase in P660s time (Fig. 2c) suggest that the transition zone thickness anomaly results primarily from the shoaling of the 410-km discontinuity.

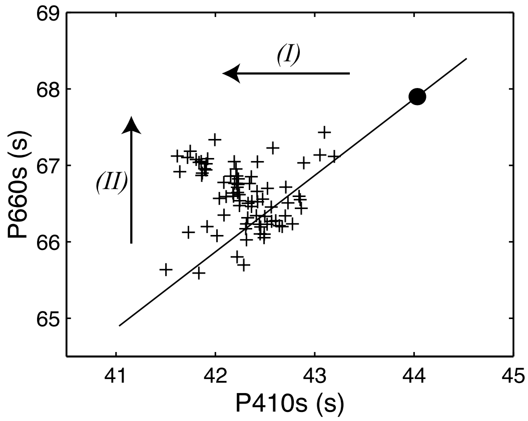

Fig. 4. Correlation between the arrival times of P410s and P660s phases (crosses). The line shown has a slope of 1 and satisfies the predicted times for the iasp91 model (dot). Variations in the P410s and P660s times along the line of unit slope are contributed by mantle structure above 410 km depth. Correction for relative travel time delays across the array does not remove the mean velocity anomaly. The offsets between the data points and the line provide information on the thickness of the mantle transition zone. Arrows represent two end-member models in which the increase in P660s–P410s differential time relative to iasp91 is caused by (I) a shoaling of the 410-km discontinuity, or (II) a deepening of the 660-km discontinuity.

4. Discussion

The transition zone structure beneath southern Africa appears unaffected by thermal upwelling in the lower mantle. Although the transition zone thickness is marginally thinner-than-normal beneath the Namaqua-Natal and Cape Fold belts, the thicker-than-normal transition zone beneath the expansive Zimbabwe and Kaapvaal cratons and the normal transition zone beneath the Bushveld province suggest that the upper mantle is not anomalously warm. The average transition zone thickness over the imaged area is ∼5 km greater than in the iasp91 average earth model. The signature of the thermal upwelling is thereby confined to the lower mantle beneath the study area [20]. We note that this observation does not rule out the possibility of upwelling of ambient mantle without large excess temperature in the transition zone beneath regions off the Zimbabwe and Kaapvaal cratons.

If temperature variation is the sole cause of the transition zone thickness anomaly beneath the study area, the thickening of the transition zone beneath the Zimbabwe and Kaapvaal cratons corresponds to a temperature reduction of ∼160 K, given Clapeyron slopes of 2.9 and −2.1 MPa/K for the 410- and 660-km discontinuities, respectively [31]. This simple explanation, however, is

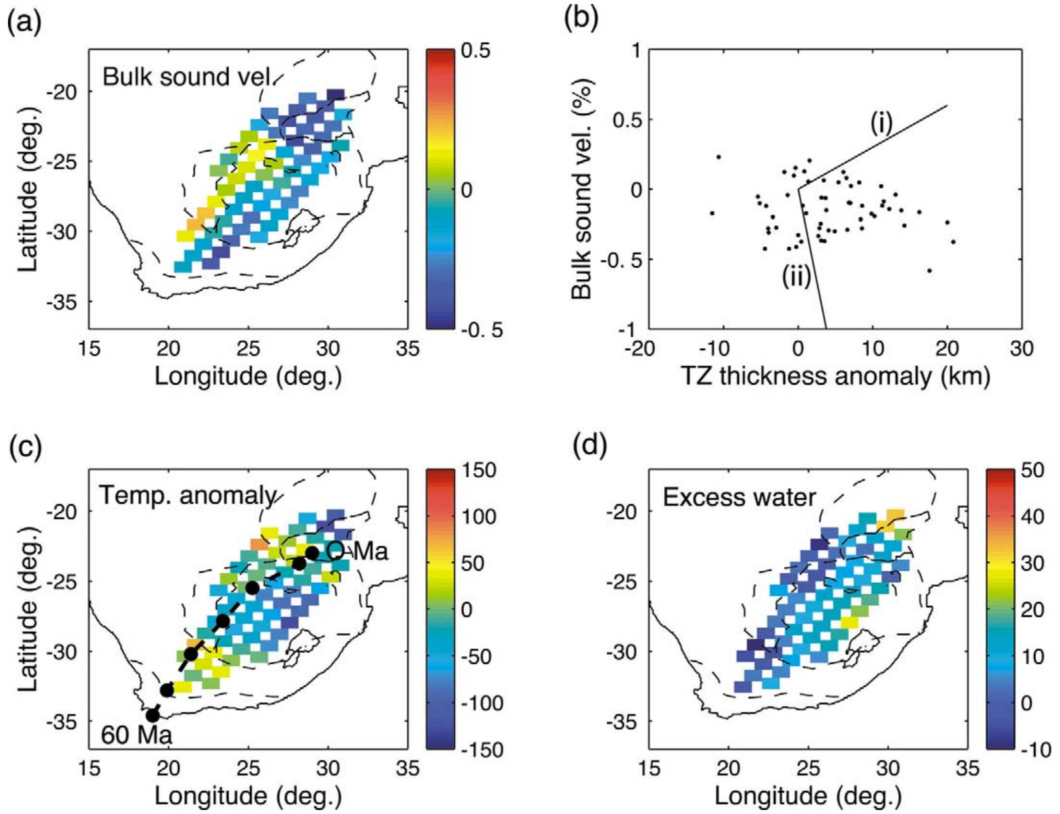

Fig. 5. (a) The bulk sound velocity perturbation is averaged over the depth range of 410 to 660 km at bins with at least 256 receiver functions in the transition zone. (b) The transition zone thickness and bulk sound velocity (dots) do not follow the predicted trends for pure thermal (i) or hydrogen (ii) effect. Temperature anomaly in the transition zone (c) and the corresponding excess water content in percent of saturation (d) are calculated from the transition zone thickness and seismic velocity. African plate motion over the past 60 Ma [53,54] is illustrated by the heavy dashed line in panel c. Dots mark 10-Ma intervals.

inconsistent with tomographically imaged seismic velocities in the transition zone. The bulk sound velocity perturbations within the transition zone, calculated from P- and S-velocity models [15,16], do not follow the expected correlation between velocity anomaly and transition zone thickness variation from the thermal effect (Fig. 5); the bins with the thickest transition zone are associated with generally low average bulk sound velocities. In the following sections we examine the individual effects of mantle composition and temperature on the phase transformations identified with the seismic discontinuities in order to assess the causes of the variations in the transition zone in the presence of continental keels and the presumed lower mantle upwelling.

4.1. Compositional and thermal implications

Compositional variations, such as iron enrichment, can elevate the 410-km discontinuity. The effect of moderate iron enrichment on the olivine–wadsleyite phase transformation is small, however, relative to the variations in the depth to the discontinuity observed beneath the study area. A 14% increase in Fe content is calculated to reduce the depth to the 410-km discontinuity by 3–4 km [32]. Furthermore, the bulk of the cratons are depleted in iron except for the Bushveld province (Fig. 1), where iron enrichment is suggested to be responsible for the lower seismic velocities observed in the P- and S-wave tomographic inversions [15,16]. The fact that the transition zone thickness beneath the Bushveld province does not significantly differ from the normal value is consistent with the predicted relatively small influence of iron on the depth of the phase transformation.

Water is another plausible compositional agent that could affect the depths to the 410- and 660-km seismic discontinuities. Theoretical calculations predict that rich H_2O content within the olivine–wadsleyite transformation stabilizes β-spinel, resulting in a shallower and broader 410-km discontinuity than in the mantle of normal H_2O value [33]. A mantle source with 500 ppm H_2O, for example, is calculated to have an α–β phase transformation that averages 8 km shallower than a dry mantle source. Recent laboratory results confirm that the presence of water within the mantle will reduce the depth to the 410-km discontinuity by up to 8 km [34]. The laboratory results suggest, however, that water will sharpen, not broaden, the 410-km seismic discontinuity. In a water-saturated mantle, the α–β phase transformation occurs over an interval of 9 km. We observed P410s with a dominant wavelength of ∼15 km beneath the Zimbabwe and Kaapvaal cratons. Observation of the converted phases at this wavelength indicates that the α–β phase transformation beneath the cratons occurs over a depth interval of less than ∼15 km, consistent with the laboratory results and the results of Gao et al. [20], who reported an ∼8-km discontinuity. Additionally, the spinel–postspinel phase boundary (the 660-km discontinuity) has been found to move to greater depth by ∼6 km in hydrous conditions compared to that in a dry mantle [35].

The transition zone is a plausible major water reservoir within the mantle. The water storage potential per unit mass of $(Mg,Fe)_2SiO_4$ wadsleyite and ringwoodite is 2–3 wt% [36,37]. Given experimental constraints on water partitioning in the $MgO–SiO_2–H_2O$ system [38], a pyrolitic mantle transition zone could store up to 1.3–2 wt% H_2O. In the early Earth's mantle, the transition zone was likely to be relatively enriched in water [39]. Petrological results indicate that Archaean komatiites from southern Africa contain considerable quantities of water (>4% wt), suggesting the presence of water in their sources [40,41]. The south African cratons were formed rapidly in the presence of subduction zones [5,6] and subducting lithosphere may supply water to the transition zone [42,43]. A cold transition zone would be a particularly likely place for accumulation of excess water due to higher water solubility than in ambient mantle [44,45], especially during the Archaean. Water exsolution below 660 km and heavy melts above the 410-km discontinuity could prevent convective mixing of water throughout the mantle over time [46].

Excess water and other moderate compositional anomalies in the Earth's mantle, however, also fail to fully explain the 20-km increase in the transition zone thickness and the seismic velocities in the transition zone beneath the study area (Fig. 5). A water-saturated mantle would reduce the bulk sound velocities of wadsleyite and ringwoodite by ∼3.7% [47] and ∼4.0% [48], respectively, several times greater than the observed velocity anomaly. For comparison, a 600–800-K reduction in mantle temperature in the transition zone would increase seismic velocity by a similar magnitude [49]. The seismic velocity of the mantle transition zone could thus be strongly influenced by water enrichment and a water-rich and cold transition zone may be difficult to image tomographically because of the opposite effects of higher water content and lower temperature on seismic velocities. The same consideration should also be given in the interpretation of seismic velocity in shallower mantle [50] beneath continental keels.

We suggest that a water-enriched and cold transition zone best fits both the observed transition zone anomaly and velocity values. Assuming that temperature and water content are the dominant causes of variations in transition zone thickness and seismic velocity, we have:

$$\begin{aligned} \delta H_{tz} &= a\Delta T + b\Delta \mathrm{OH} \\ \delta V_{tz} &= c\Delta T + d\Delta \mathrm{OH} \end{aligned} \quad (1)$$

where δH_{tz} and δV_{tz} are variations in transition zone thickness and bulk sound velocity, respectively, relative to an average earth. ΔT and ΔOH are excess temperature in K and percent of water saturation, respectively. For Clapeyron slopes of 2.9 and −2.1 MPa/K for the 410- and 660-km discontinuities [31], a equals −0.13 km/K. Other constants are b (0.14 km per percent of water saturation [34,35]), c (-6×10^{-5} l/K [49]), and d (-0.038 per percent of water saturation [47,48]). Two simplifications in the equation require further experimental constraints: the change in the depth of the phase transition is likely a non-linear function of water content [33]; and water solubility is a function of temperature [44,45]. Assumptions in tomographic inversions (e.g. ray approximation of finite-frequency travel times and damping) introduce errors in the estimates of seismic velocities. To minimize observational errors in transition zone thickness and seismic velocities, we apply the above equation only to bins with at least 256 traces in the transition zone (Fig. 5). This stringent requirement effectively removes bins not directly beneath the array. The remaining bins are well sampled by crossing body wave ray paths and have estimated transition zone thicknesses within ±3 km. With these caveats and the safeguard, Eq. 1 yields that the transition zone anomaly beneath the Zimbabwe and Kaapvaal cratons can be explained by a combination of $\sim$100 K temperature reduction and an excess water content of 20–35% saturation (0.3–0.7 wt% H_2O, assuming that the water saturation limit for a pyrolitic transition zone is 1.3–2 wt%). The average level of excess water content in the transition zone beneath the study area is $\sim$8% saturation, while the average temperature reduction is $\sim$25 K.

Water may also provide a plausible explanation that reconciles the observed transition zone thickness and high attenuation (low Q) in the transition zone beneath the study area [4], although the latter is resolved at much greater length scales. Water enhances the mobility of defects and thus seismic attenuation in olivine [50]. The same theoretical consideration also suggests that water enhances attenuation in wadsleyite and ringwoodite (Karato, personal communication), though experimental constraints are currently unavailable. This interpretation implies that the effect of excess water in the transition zone is greater than that of temperature reduction. A more detailed attenuation study at the scales of the observed transition zone variation is needed to test this inference.

4.2. Geodynamic constraints

Numerical simulations of small-scale convection in the upper mantle provide important insights into the geodynamic processes that are associated with the transition zone thickness anomaly [51]. It has been suggested that small-scale edge-driven convection may produce cold downwellings adjacent to boundaries of lithosphere with large thermal contrast [13,14]. One characteristic of the predicted downwelling is that the temperature anomaly is largest near the base of the thick lithosphere and much reduced at great depth. The isolated shoaling of the 410-km discontinuity with no detectable corresponding deepening of the 660-km discontinuity near the boundary between the Kheis thrust belt and the Namaqua-Natal belt appears consistent with this scenario.

Small-scale downwelling, however, cannot explain the transition zone thickness anomaly beneath the Kaapvaal and Zimbabwe cratons. In models of small-scale convection that incorporate the transition zone phase transformations, downwelling is limited in the upper mantle [14,52]. Consequently, cold mantle accumulates and spreads above the 660-km discontinuity. For a moving plate, the downwelling is expected to leave a track of cold mantle within the transition zone in the direction of plate motion (Fig. 6a) [53,54]. Thus, if the downwelling mantle has temperature and compositional anomalies large enough to cause the variations in the depth to the 660-km discontinuity, it would produce a swath of anomalously thick transition zone that runs parallel to the track of plate motion. No such feature is observed (Fig. 2). The transition zone thickness anomalies beneath the Kaapvaal and Zimbabwe cratons are confined, with no apparent skewness in the direction of plate motion. The spatial correlation between surface geology and the transition zone structure requires that the thermal and compositional heterogeneity responsible for the 20-km increase in transition zone thickness move with the lithosphere. This implies that the cratonic keels extend into the transition zone (Fig. 6b). If thermal downwelling exists beneath the study area, its temperature

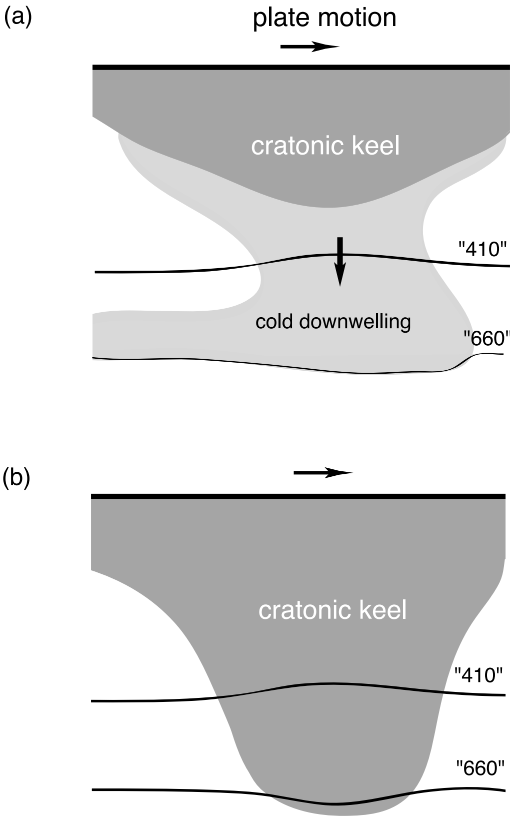

Fig. 6. Schematic illustration of two scenarios of the transition zone structure and cratonic keels. (a) The cratonic keel is shallower than 400 km depth. Cold downwelling mantle accumulates above the 660-km discontinuity, causing a track of deeper-than-normal 660-km discontinuity in the direction of plate motion. (b) The cratonic keel penetrates the transition zone. The shoaling of the 410-km discontinuity and the deepening of the 660-km discontinuity are due to a lower-than-normal temperature and a higher-than-normal water content of the cratonic keel.

anomaly at the 660-km discontinuity must be below the levels detectable to the method used in this study ($\Delta T \sim 60$ K for a Clapeyron slope of -2.1 MPa/K for the post-spinel phase transformation).

5. Conclusions

Variations in the transition zone structure beneath southern Africa correlate geographically with the surface geology and recent P- and S-wave imaging of the upper mantle beneath southern Africa. Patches of high seismic velocities beneath the Zimbabwe and Kaapvaal cratons in the upper 200–300-km mantle correspond spatially to the 20-km thicker-than-normal transition zone. A relatively cold ($\Delta T \sim 100$ K) and water-rich transition zone (ΔOH$\sim$20–35% saturation) best explains the seismic velocities and transition zone thickness anomaly beneath the cratons. Because the spatial correlation between surface geology and the transition zone structure requires that the thermal and compositional heterogeneity responsible for the 20-km increase in transition zone thickness move with the lithosphere – and there is no apparent thickness anomaly opposite the direction of plate motion – we conclude that the cratonic keels extend into the transition zone. How far cratonic roots penetrate into the mantle remains unknown, but evidence for a depressed 660-km discontinuity beneath the cratons indicates that the roots extend to at least the base of the upper mantle. Our findings demonstrate the need to closely consider the effect of water content on seismic velocities and transition zone thickness beneath deep continental roots. The results fundamentally constrain geodynamic models that seek to explain mantle dynamics, the plate tectonics of the African continent, and the depth and the stability of continental keels over geologic time.

Acknowledgements

We thank participants in the Kaapvaal Project, along with Matt Fouch and Jeffrey Gu for thoughtful reviews of the original manuscript. M. Fouch and David James kindly provided the tomographic models used in this study and Sue Webb provided the digital location of geologic provinces. This work was supported by the US NSF.***[SK]***

References

[1] C. Lithgow-Bertelloni, P.G. Silver, Dynamic topography plate driving forces and the African Superswell, Nature 395 (1998) 269–273.

[2] R.D. vanderHilst, S. Widiyantoro, E.R. Engdahl, Evidence for deep mantle circulation from global tomography, Nature 386 (1997) 578–584.

[3] S. Ni, D.V. Helmberger, Seismological constraints on the South African superplume; could be the oldest distinct structure on earth, Earth Planet. Sci. Lett. 206 (2003) 119–131.

[4] B. Romanowicz, Y. Gung, Supperplumes from the core-mantle boundary to the lithosphere implications for heat flux, Science 296 (2002) 513–517.

[5] M.J. de Wit, C. Roering, R.J. Hart, R.A. Armstrong, C.E.J. de Ronde, R.W.E. Green, M. Tredoux, E. Peberdy, R.A. Hart, Formation of an Archaean continent, Nature 357 (1992) 553–562.

[6] S.W. Parman, J.C. Dann, T.L. Grove, The production of Barberton komatiites in an Archaean subduction zone, Geophys. Res. Lett. 28 (2001) 2513–2516.

[7] M.Q.W. Jones, Heat flow in the Witwatersrand Basin and environs and its significance for the South African shield geotherm and lithosphere thickness, J. Geophys. Res. 93 (1988) 3243–3260.

[8] T.H. Jordan, Mineralogies, densities and seismic velocities of garnet lherzolites and their geophysical implications, in: F.R. Boyd et al. (Eds.), The Mantle Sample: Inclusions in Kimberlites and Other Volcanics, AGU, Washington, DC, 1979, pp. 1–14.

[9] T.H. Jordan, The continental tectosphere, Rev. Geophys. Space Phys. 13 (1975) 1–12.

[10] Y. Gu, A.M. Dziewonski, C.B. Agee, Global de-correlation of the topography of transition zone discontinuities, Earth Planet. Sci. Lett. 157 (1998) 57–67.

[11] A. Li, K.M. Fischer, M.E. Wysession, T.J. Clarke, Mantle discontinuities and temperature under the North Americancontinental keel, Nature 395 (1998) 160–163.

[12] J. Ritsema, H. van Heijst, J.H. Woodhouse, Complex shear wave velocity structure imaged beneath Africa and Iceland, Science 286 (1999) 1925–1928.

[13] S.D. King, D.L. Anderson, Edge-driven convection, Earth Planet. Sci. Lett. 160 (1998) 289–296.

[14] S.D. King, J. Ritsema, African hot spot volcanism small-scale convection in the upper mantle beneath cratons, Science 290 (2000) 1137–1140.

[15] D.E. James, M.J. Fouch, J.C. VanDecar, S van der Lee, and Kaapvaal Seismic Group, Tectospheric structure beneath southern Africa, Geophys. Res. Lett. 28 (2001) 2485–2488.

[16] D.E. James, M.J. Fouch, Formation and evolution of Archaean cratons: insights from southern Africa, in: C.M.R. Fowler, C. Ebinger, C.J. Hawkesworth (Eds.), Early Earth: Physical, Chemical and Biological Development. Geol. Soc. London Spec. Publ. 199 (2002) 1–26.

[17] L. Liu, Phase transformations and the constitution of the deep mantle, in: M.W. McElhinny (Ed.), The Earth: Its Origin, Structure and Evolution, Academic Press, San Diego, CA, 1979, pp. 177–202.

[18] C.R. Bina, Mantle discontinuities, Rev. Geophys. 29 (1991) 783–793.

[19] J. Revenaugh, T.H. Jordan, Mantle layering from ScS reverberations; 2, the transition zone, J. Geophys. Res. 96 (1991) 19,763–19,780.

[20] S.S. Gao, P.G. Silver, K.H. Liu, the Kaapvaal Seismic Group, Mantle discontinuities beneath Southern Africa, Geophys. Res. Lett. 29 (2002) 1291–1294.

[21] C.A. Langston, Structure under Mount Rainer, Washington, inferred from teleseismic body waves, J. Geophys. Res. 84 (1979) 4749–4762.

[22] C.J. Ammon, The isolation of receiver effects from teleseismic P waveforms, Bull. Seismol. Soc. Am. 81 (1991) 2504–2510.

[23] T.K. Nguuri, J. Gore, D.E. James, S.J. Webb, C. Wright, T.G. Zengeni, O. Gwavana, J.A. Snoke, Kaapvaal Seismic Group, Crustal structure beneath southern Africa and its implications for the formation and evolution of the Kaapvaal and Zimbabwe cratons, Geophys. Res. Lett. 28 (2001) 2501–2504.

[24] J.C. VanDecar, R.S. Crosson, Determination of teleseismic relative phase arrival times using multi-channel cross correlation and least squares, Bull. Seismol. Soc. Am. 80 (1990) 150–169.

[25] B.L.N. Kennett, E.R. Engdahl, Travel times for global earthquake location and phase identification, Geophys. J. Int. 105 (1991) 429–466.

[26] K.G. Dueker, A.F. Sheehan, Mantle discontinuity structure beneath the Colorado Rocky Mountains and High Plains, J. Geophys. Res. 103 (1998) 7153–7169.

[27] Y. Shen, A.F. Sheehan, K.G. Dueker, C. de Groot-Hedlin, H. Gilbert, Mantle discontinuity structure beneath the southern East Pacific Rise from P-to-S converted phases, Science 280 (1998) 1232–1235.

[28] E.R. Kanasewich, C.D. Hemmings, T. Alpaslan, *N*th-root stack nonlinear multichannel filter, Geophysics 38 (1973) 327–338.

[29] B. Efron, G. Gong, A leisurely look at the bootstrap, the jackknife, and cross-validation, Am. Stat. 37 (1983) 36–48.

[30] Y. Shen, J. Blum, Seismic evidence for accumulated oceanic crust above the 660-km discontinuity beneath southern Africa, Geophys, Res. Lett. 30 (2003) doi: 10.1029/2003GL017991.

[31] C.R. Bina, G. Helffrich, Phase transition Clapeyron slopes and transition zone seismic discontinuity topography, J. Geophys. Res. 99 (1994) 15,853–15,860.

[32] D.J. Weidner, Y. Wang, Phase transformations: implications for mantle structure, in: S. Karato et al. (Eds.), Earth's Deep Interior: Mineral Physics and Tomography from the Atomic to the Global Scale, AGU, Washington, DC, 2000, pp. 215–236.

[33] B.J. Wood, The effect of H_2O on the 410-km seismic discontinuity, Science 268 (1995) 74–76.

[34] J. Chen, T. Inoue, H. Yurimoto, D.J. Weidner, Effect of water on olivine-wadsleyite phase boundary in the $(Mg, Fe)_2SiO_4$ system, Geophys. Res. Lett. 29 (2002) 1875–1878.

[35] Y. Higo, T. Inoue, T. Irifune, H. Yurimoto, Effect of

water on the spinel-postspinel transformation in Mg_2SiO_4, Geophys. Res. Lett. 28 (2001) 3505–3508.
[36] E. Ohtani, M. Toma, K. Litasov, T. Kubo, A. Suzuki, Stability of dense hydrous magnesium silicate phases and water storage capacity in the transition zone and lower mantle, Phys. Earth Planet. Inter. 124 (2001) 105–117.
[37] D.L. Kohlstedt, H. Keppler, D.C. Rubie, Solubility of water in the α, β, and γ phases of (Mg, Fe)2SiO4, Contrib. Mineral. Petrol. 123 (1996) 345–357.
[38] N. Bolfan-Casanova, H. Keppler, D.C. Rubie, Water partitioning between nomincally anhydrous minerals in the MgO-SiO2-H2O system up to 24 GPa: implications for the distribution of water in the Earth's mantle, Earth Planet. Sci. Lett. 182 (2000) 209–221.
[39] T. Kawamoto, R.L. Hervig, J.R. Holloway, Experimental evidence for a hydrous transition zone in the early Earth's mantle, Earth Planet. Sci. Lett. 142 (1996) 587–592.
[40] R.W. Carlson, F.R. Boyd, S.B. Shirey, P.E. Janney, T.L. Grove, S.A. Bowring, M.D. Schmitz, J.C. Dann, D.R. Bell, J.J. Gurney, S.H. Richardson, M. Tredoux, A.H. Menzies, D.G. Pearson, R.J. Hart, A.H. Wilson, D. Moser, Continental growth, preservation, and modification in southern Africa, GSA Today 10 (2000) 1–7.
[41] T.L. Grove, S.W. Parman, J.C. Dann, Conditions of magma generation for Archaean komatiites from the Barberton Mountainland, South Africa, in: Y. Fei, C.M. Bertka, B.O. Mysen (Eds.), Mantle Petrology: Field Observations and High Pressure Experimentation: A Tribute to Francis R. (Joe) Boyd, The Geochem. Soc., Houston, TX, 1999, pp. 155–167.
[42] G. Nolet, A. Zielhus, Low S velocities under the Tornquist-Teisseyre zone; evidence for water injection into the transition zone by subduction, J. Geophys. Res. 99 (1994) 15813–15820.
[43] L.-G. Liu, Phase transformation in serpentine at high pressures and temeperatures and implications for subducting lithosphere, Phys. Earth Planet. Inter. 42 (1986) 255–262.
[44] Q. Williams, R. Hemley, Hydrogen in the deep earth, Annu. Rev. Earth Planet. Sci. 29 (2001) 365–418.
[45] E. Ohtani, H. Mizobata, H. Yurimoto, Stability of dense hydrous magnesium silicate phase in the system Mg_2SiO_4-H_2O and $MgSiO_3$-H_2O at pressure up to 27 GPa, Phys. Chem. Miner. 27 (2000) 533–544.
[46] D. Bercovici, S. Karato, Whole-mantle convection and the transition-zone water filter, Nature 245 (2003) 39–44.
[47] H. Yusa, T. Inoue, Compressibility of hydrous wadsleyite (beta-phase) in Mg_2SiO_4 by high-pressure X ray diffraction, Geophys. Res. Lett. 24 (1997) 1831–1834.
[48] T. Inoue, D.J. Weidner, P.A. Northrup, J.B. Parise, Elastic properties of hydrous ringwoodite (γ-phase) in Mg_2SiO_4, Earth Planet. Sci. Lett. 160 (1998) 107–113.
[49] S. Karato, Importance of anelasticity in the interpretation of seismic tomography, Geophys. Res. Lett. 20 (1993) 1623–1626.
[50] S. Karato, H. Jung, Water, partial melting and the origin of the seismic low velocity and high attenuation zone in the upper mantle, Earth Planet. Sci. Lett. 157 (1998) 193–207.
[51] A. Lenardic, W.M. Kaula, Mantle dynamics and the heatflow into the Earth's continents, Nature 378 (1995) 709–711.
[52] P.J. Tackley, On the stability of phase transitions and viscosity layering to induce long wavelength heterogeneity in the mantle, Geophys. Res. Lett. 23 (1996) 1985–1988.
[53] R.D. Müller, J.Y. Royer, L.A. Lawver, Revised plate motions relative to the hotspots from combined Atlantic and Indian Ocean hotspot tracks, Geology 21 (1993) 275–278.
[54] W.W. Hay, R. DeConto, C.N. Wold, K.M. Wilson, S. Voight, M. Schulz, A. Wold-Rossby, W.C. Dullo, A.B. Ronov, A.N. Balukhovsky and E. Soeding, Alternative global Cretaceous paleogeography, in: C. Johnson, E. Barrera (Eds.), Evolution of Cretaceous Ocean–Climate Systems, GSA Special Paper 332 (1999) 1–47.